

PREDICTION AND EVALUATION OF EDDY-VISCOSITY  
MODELS FOR FREE MIXING \*

By V. Zakkay, R. Sinha, and S. Nomura  
New York University

SUMMARY

Analysis for the turbulent mixing of free jets is presented in this paper and compared to recent experimental results. A turbulent mass diffusion model is presented and is based on the concentration potential core. The model yielded good results when compared with the experimental results except for low-speed flows where few experimental data are available.

A review of recent experimental results verifies again that the three diffusion processes in turbulent mixing are interrelated; however, no single diffusion model may be used for all three processes. This is especially true when pressure gradients are present in the flow field. It is shown that even though momentum diffusion is significantly affected by pressure gradients, mass diffusion is not.

It is further indicated that the mass diffusion model has been derived and is based on the accurate correlations of experimental results obtained for the concentration potential core. Similar techniques may be used in deriving an expression for the momentum and thermal diffusion coefficients. These expressions would be more complicated since they would have to take care of boundary layer at the start of the mixing region.

Finally, a comparison of the analyses, using this particular model and Ferri's model, with available experimental results is made.

INTRODUCTION

The problem of free turbulent mixing with large density gradients has been an area of considerable interest and ever increasing practical importance in the past decade. Problems of constant density mixing may be traced back as far as the 1930's. These types of problems have a wide variety of applications and have been used for wakes, rocket planes, supersonic combustion, nuclear core reactions, and so forth.

---

\* This research was sponsored in part by the Aerospace Research Laboratories, Air Force Systems Command, United States Air Force, Wright-Patterson Air Force Base, Ohio, under Contract F-33615-68-C-1184 and in part by NASA International Fellowships.

In reference 1, the Prandtl eddy-viscosity model for constant density flow was extended to the variable density flow. However, as pointed out in reference 2, this model fails when the mass flux of each stream is equal. Ting and Libby (ref. 3) determined the compressibility factor for the Prandtl model using their transformation, while Donaldson and Gray (ref. 4) and Peters (ref. 5) obtained the compressibility factor empirically. These models, however, fail also when the velocity of each stream is equal, since the Prandtl model becomes zero. Zakkay, Krause, and Woo (ref. 6) developed the eddy-viscosity model in terms of the center-line velocity and velocity half-radius. Schetz (ref. 7) extended the Clauser model (ref. 8) to the axisymmetric wake which was expressed in terms of mass defect across the wake.

Each of all these models has a constant which is chosen such that the numerical solutions of wake equations agree with the experimental data by employing the proposed eddy viscosity and appropriate constant values for turbulent Prandtl number  $Pr_t$  and turbulent Schmidt number  $Sc_t$ . Therefore, it has been found in references 2, 9, and 10 and also in the present investigation that all these models provide good predictions for certain very restricted flow conditions, but none of them is valid for the general case.

In comparison with these numerous works for the eddy viscosity, only few extensive works have been done for other transport properties, namely  $Pr_t$ ,  $Sc_t$ , and  $Le_t$  (turbulent Lewis number). In analytical and numerical investigations so far, constant values for  $Pr_t$  and  $Sc_t$  have been assumed, and several experimental studies seem to approve these assumptions of constant properties under the condition of zero pressure gradient in the mixing flow field.

In reference 11, Forstall and Shapiro determined  $Le_t = 1.0$  and  $Pr_t = Sc_t = 0.7$  using the data of air-to-air mixing measured at very low speed. Zakkay et al. (ref. 6) carried out extensive measurements for the turbulent mixing of high-speed coaxial jets comprised of several dissimilar gases. For hydrogen and air mixing,  $Sc_t = 0.8$  to  $2.0$  and  $Le_t = 0.9$  to  $1.2$  have been concluded. Chriss (ref. 12) measured very detailed profiles in mixing flows of high-speed coaxial air and hydrogen jets and obtained  $Le_t = 1.0$ . The accuracy of these experimental data has been checked by Zelazny, Morgenthaler, and Herendeen (ref. 9) and Harsha (ref. 10) by means of constant-momentum integral check and was found to be very good. Peters, Chriss, and Paulk (ref. 13) have shown for one case of hydrogen and air mixing measured by Chriss that  $Pr_t = Sc_t = 0.85$  is approximately valid. Zelazny et al. (ref. 9) also calculated  $Sc_t$  for four cases of Chriss' data (ref. 12) and confirmed the result obtained by Peters et al. (ref. 13).

It is difficult at this time to generalize and to derive equations for a single application; however, some basic conclusions have been reached from past research efforts. For example, the authors have indicated previously that the mixing which occurs between two coaxial streams depends largely on their initial energy and their transfer phenomena

in the mixing region. Therefore, differentiation must be made between jets where momentum diffusion is the controlling mechanism and jets where mass diffusion, or thermal diffusion, is the controlling mechanism. Theoretical treatment of the problem is impossible since turbulent transport properties for the three diffusion processes are not yet available. Reference 6 has attempted to deduce such turbulent transport coefficients from mass diffusion experiments.

Similar attempts have been made in wakes to deduce momentum diffusion coefficients; however, no single model has been capable of analyzing the entire range of flow fields. In addition to the complications of the unknown transport properties, in several problems, the pressure field is not constant, and therefore complicates the analysis further. For instance, references 14 and 15 have indicated that pressure gradients do not affect mass diffusion; however, momentum diffusion is significantly affected. These regions of varying pressure gradients are present close to the exit of the jets and are directly responsible for the discrepancies among constant-pressure analyses. Results of mixing with pressure gradients, in reference 15, indicate a large discrepancy between theory and experiments for momentum diffusion, although good agreement exists for mass diffusion.

Therefore, since the topic under discussion is complex and cannot be described in terms of one single model, the present paper will concentrate on the mixing of coaxial jets with special emphasis on mass-diffusion processes. At first a description of the model used for mass diffusion will be derived (see fig. 1) and then the predictions of this model are compared with several of the test cases supplied by the organizers of the Langley working conference on free turbulent shear flows.

#### SYMBOLS

$c_p$	specific heat at constant pressure
$\bar{c}_p$	normalized specific heat with respect to $c_{pe}$
$\bar{c}_{pk}$	normalized specific heat of kth gas; $k = 1$ corresponds to inner jet gas and $k = 2$ corresponds to outer jet gas
$D_j$	inner jet nozzle diameter
$D_t$	turbulent diffusion coefficient
$H$	total enthalpy of gas

$h_k$	static enthalpy of kth gas
$Le_t$	turbulent Lewis number
$M$	local Mach number
$N$	total number of grid points in $\tau$ -direction
$n$	concentration decay exponent along center line
$p$	static pressure
$Pr_t$	turbulent Prandtl number
$R$	gas constant
$Re$	Reynolds number
$r$	radial coordinate
$\bar{r}$	normalized radial coordinate with respect to $r_j$
$r_j$	radius of inner jet nozzle
$r_{mc}$	concentration half-radius defined so that $Y_j = \frac{Y_{j\phi}}{2}$ at $r = r_{mc}$
$\bar{r}_{mc}$	normalized half-radius with respect to $r_j$
$r_{mu}$	velocity half-radius defined so that $u = \frac{u_{\phi} + u_e}{2}$ at $r = r_{mu}$
$Sc_t$	turbulent Schmidt number
$T$	temperature
$\bar{T}$	normalized temperature with respect to $T_e$
$u$	axial component of velocity
$\bar{u}$	normalized axial velocity with respect to $u_e$

$v$	radial component of velocity
$\bar{v}$	nondimensional radial velocity
$W$	ratio of molecular weights, $W_j/W_e$
$\bar{W}$	normalized molecular weight with respect to $W_e$
$x$	axial coordinate
$x_i$	initial value of $x$ to start computation
$x_0$	concentration potential core length
$\bar{x}$	normalized axial coordinate with respect to $r_j$
$\bar{x}_0$	normalized $x_0$ with respect to $r_j$
$\tilde{x}$	normalized axial coordinate with respect to $x_0$
$Y_j$	mass concentration of inner jet gas
$Y_k$	mass concentration of $k$ th gas; $k = 1$ corresponds to inner jet gas, and $k = 2$ corresponds to outer jet gas
$\zeta$	transformed axial coordinate defined as $\frac{1}{4} \int_{\bar{x}_i}^{\bar{x}} Re^{-1} d\bar{x}$
$\epsilon$	eddy viscosity
$\gamma$	specific-heat ratio
$\lambda$	mass-flow ratio defined as $\frac{\rho_j u_j}{\rho_e u_e}$
$\Psi$	modified stream function defined by equation (7)
$\phi_{u_t}$	normalized center-line velocity defined by $\frac{u_e - u_t}{u_e - u_j}$
$\xi$	transformed axial coordinate defined as $2 \int_0^{\bar{x}} \overline{(\rho D_t)} d\bar{x}$

$\rho$	density
$\bar{\rho}$	normalized density with respect to $\rho_e$
$\tau$	modified stream function defined as $\left(\int_0^{\bar{r}} \bar{\rho} \bar{u} \bar{r} d\bar{r}\right)^{0.5}$
$\tau_t$	turbulent shear stress
$\mu_t$	turbulent viscosity
$\overline{(\rho D_t)}$	normalized value of $\rho D_t$ with respect to $\rho_j u_j r_j$
$\overline{(\rho u)}$	normalized value of $\rho u$ with respect to $\rho_j u_j$
$\overline{(\rho v)}$	normalized value of $\rho v$ with respect to $\rho_e u_e$

Subscripts:

$\epsilon$	center-line values
e	external conditions
i	initial conditions
j	inner jet conditions

## THEORETICAL ANALYSIS

### Basic Equations and Turbulent Diffusion Coefficient

The governing equations for the mean turbulent flow properties in coaxial mixing with axial pressure gradient can be described as follows:

Conservation of mass:

$$\frac{\partial}{\partial x}(\rho u) + \frac{1}{r} \frac{\partial}{\partial r}(\rho v r) = 0 \quad (1)$$

Conservation of momentum:

$$\rho u \frac{\partial u}{\partial x} + \rho v \frac{\partial u}{\partial r} = \frac{1}{r} \frac{\partial}{\partial r} \left( \rho \epsilon r \frac{\partial u}{\partial r} \right) - \frac{dp}{dx} \quad (2)$$

Conservation of energy:

$$\rho u \frac{\partial H}{\partial x} + \rho v \frac{\partial H}{\partial r} = u \frac{dp}{dx} + \frac{1}{r} \frac{\partial}{\partial r} \left( \frac{\rho \epsilon}{Pr_t} r \frac{\partial H}{\partial r} + \frac{Pr_t - 1}{Pr_t} \rho \epsilon r u \frac{\partial u}{\partial r} + \frac{Le_t - 1}{Pr_t} \rho \epsilon r \sum_k h_k \frac{\partial Y_k}{\partial r} \right) \quad (3)$$

Conservation of species:

$$\rho u \frac{\partial Y_j}{\partial x} + \rho v \frac{\partial Y_j}{\partial r} = \frac{1}{r} \frac{\partial}{\partial r} \left( \frac{\rho \epsilon}{Sc_t} r \frac{\partial Y_j}{\partial r} \right) \quad (4)$$

where the following conditions were assumed:

- (1) The flow is chemically frozen.
- (2) The radial pressure gradient is not existing.
- (3) The streamwise pressure gradient is supposed to exist and therefore the external flow conditions could be variable.

In references 16 and 17, equations (1) to (4) are solved for the axisymmetric coaxial jet mixing with the assumptions of  $dp/dx = 0$ ,  $Pr_t = Sc_t = Le_t = 1.0$ , and step initial profiles for velocity, enthalpy, and concentration. Obviously these assumptions reduce those equations to a single equation and the solution can be applicable for any flow properties. As for these assumptions, however, the transport coefficients  $Pr_t$ ,  $Sc_t$ , and  $Le_t$  are generally not equal to unity, and the initial profiles are not always step profiles because of boundary layers developed on the jet nozzle wall. The exact application of this solution is possible only for the species equation involving the turbulent diffusion coefficient, for which the initial profile can be assumed correctly to be a step profile and in which other transport properties are not directly involved. Furthermore, even if the axial pressure gradients exist, the mass diffusion will not be affected significantly as shown experimentally in references 6, 14, and 15 and in the present experiment, since the pressure gradient affects the concentration indirectly through velocity and temperature field as seen in equation (4). Therefore, the solutions as obtained in references 16 and 17 can be employed exactly only for the species equation involving the turbulent diffusion coefficient in the mixing with axial pressure gradients.

The species equation with the diffusion coefficient is

$$\rho u \frac{\partial Y_j}{\partial x} + \rho v \frac{\partial Y_j}{\partial r} = \frac{1}{r} \frac{\partial}{\partial r} \left( \rho D_t r \frac{\partial Y_j}{\partial r} \right) \quad (5)$$

where the initial conditions at  $x = 0$  are

$$Y_j = 1 \quad (\text{for } 0 \leq r \leq r_j)$$

$$Y_j = 0 \quad (\text{for } r_j < r < \infty)$$

and the boundary conditions are

$$\frac{\partial Y_j}{\partial r} = 0 \quad (\text{at } r = 0)$$

$$Y_j = 0 \quad (\text{at } r \rightarrow \infty)$$

Applying the modified von Mises transformation, Kleinstein obtained the exact solution for the linearized boundary-layer equation in reference 17. Employing the same method, the species equation can be solved as follows:

Equation (5) is transformed to

$$\frac{\partial Y_j}{\partial x} = \frac{4}{\Psi} \frac{\partial}{\partial \Psi} \left[ \overline{(\rho D_t)} \overline{(\rho u)} \bar{r}^2 \left( \frac{1}{\Psi} \frac{\partial Y_j}{\partial \Psi} \right) \right] \quad (6)$$

by the transformation terms:

$$\left. \begin{aligned} \bar{x} &= \frac{x}{r_j} \\ \frac{\partial}{\partial \bar{r}} \left( \frac{\Psi}{2} \right)^2 &= \overline{(\rho u)} \bar{r} \\ \frac{\partial}{\partial x} \left( \frac{\Psi}{2} \right)^2 &= -\overline{(\rho v)} \bar{r} \end{aligned} \right\} \quad (7)$$

Neglecting the fourth-order term in the Taylor series expansion of

$$\left[ \overline{(\rho D_t)} \overline{(\rho u)} \bar{r}^2 \right]_{\bar{x}, \Psi} = \left[ \overline{(\rho D_t)} \right]_{\bar{x}, 0} \frac{\Psi^2}{2} + O(\Psi^4)$$

the species equation (6) reduces to the linear form in  $\xi, \Psi$ -plane as

$$\frac{\partial Y_j}{\partial \xi} = \frac{1}{\Psi} \frac{\partial}{\partial \Psi} \left( \Psi \frac{\partial Y_j}{\partial \Psi} \right)$$

where  $\xi$  is defined as  $\xi = 2 \int_0^{\bar{x}} \overline{(\rho D_t)} d\bar{x}$ .

Assuming a step initial profile, the solution of this well-known heat-conduction equation can be expressed along the center line by

$$Y_{j_t} = 1 - \exp \left( - \frac{\Psi_j^2}{4\xi} \right) \quad (8)$$

where  $\Psi_j$  is  $\sqrt{2}$  by the definition given in equation (7). In the far wake region as  $\xi \rightarrow \infty$ ,  $Y_j/Y_{j_t}$  approaches the Gaussian distribution (ref. 6) as

$$\frac{Y_j}{Y_{j\zeta}} = \exp\left(-\frac{\Psi^2}{4\xi}\right) \quad (9)$$

These solutions (eqs. (8) and (9)) can be used to introduce the diffusion model in a way similar to that developed in reference 6 where Zakkay et al. introduced the eddy-viscosity model.

Since  $\overline{(\rho u)} \rightarrow \frac{1}{\lambda}$  in the far wake region as  $\xi \rightarrow \infty$ ,

$$\Psi^2 = \frac{2\bar{r}^2}{\lambda}$$

and

$$\frac{Y_j}{Y_{j\zeta}} = \exp\left(-\frac{\bar{r}^2}{2\lambda\xi}\right) \quad (10)$$

Therefore, assuming the center-line concentration decay law to be  $Y_{j\zeta} = \tilde{x}^{-n} = \left(\frac{x}{x_0}\right)^{-n}$ , the concentration profile can be expressed in the physical plane by

$$Y_j = \tilde{x}^{-n} \left(1 - \tilde{x}^{-n}\right) \bar{r}^2 / \lambda \quad (11)$$

Then the asymptotic jet spread can be given by taking the limit of equation (11) as follows:

$$\lim_{\tilde{x} \rightarrow \infty} \frac{\partial \bar{r}}{\partial \tilde{x}} = \left(-\lambda \ln \frac{Y_j}{Y_{j\zeta}}\right)^{1/2} \frac{n}{2} \tilde{x}^{\left(\frac{n}{2}-1\right)}$$

Integrating this equation gives the half-radius for concentration  $r_{mc}$  in the far wake region as

$$r_{mc} = 0.833r_j \left[\lambda \left(\frac{x}{x_0}\right)^n\right]^{1/2} \quad (12)$$

Equation (12) may provide an analytical prediction of the concentration half-radius. Once the concentration profile is expressed in the physical plane by equation (11), the turbulent diffusion coefficient can be derived from the species equation inversely.

The species equation (5) is described with the aid of the continuity equation by

$$\rho D_t r \frac{\partial Y_j}{\partial r} = \int_0^r \frac{\partial(\rho u Y_j)}{\partial x} r' dr' - Y_j \int_0^r r' \frac{\partial(\rho u)}{\partial x} dr'$$

Then the diffusion coefficient along the center line can be expressed as

$$(\rho D_t)_\zeta = \left( \frac{\rho u \frac{\partial Y_j}{\partial x}}{2 \frac{\partial^2 Y_j}{\partial r^2}} \right)_\zeta \quad (13)$$

Substituting equation (11) into equation (13) gives the turbulent diffusion coefficient on the center line as follows:

$$(\rho Dt)_{\xi} = \frac{nr_j}{4\bar{x}_0} \left( \frac{r_{mc}}{\ln 2} \right)^{\frac{n-1}{n}} \lambda^{1/n} (\rho u)_{\xi} \quad (14)$$

In equation (14) there are two unknown parameters, namely  $\bar{x}_0$  and  $n$ . The decay exponent  $n$  in  $Y_{j\xi} = \bar{x}^{-n}$  has been shown to be

$$n = 2 \quad (15)$$

for high-speed jet mixing in many experiments (for example, refs. 6, 14, and 15) and also will be shown to be  $n = 2$  in the present experiment.

Now the potential core length  $\bar{x}_0$  for concentration in high-speed mixing, where  $n = 2$  is valid, should be formulated in terms of known values. The parametric investigation has shown the importance of momentum ratio at the initial exit plane on the potential core length for concentration. The typical correlation between the potential core length for concentration and the initial Mach number ratio can be seen obviously in figure 2. The Mach number ratio of two jets can be expressed by the momentum ratio as

$$\frac{\rho_j u_j^2}{\rho_e u_e^2} = \frac{\left( \frac{pu^2}{RT} \right)_j}{\left( \frac{pu^2}{RT} \right)_e} \approx \left( \frac{M_j}{M_e} \right)^2$$

since  $p_j = p_e$ . Therefore, figure 2 shows that when the momentum ratio becomes larger, the potential core length becomes longer.

These data are rearranged in figure 3, from which the correlation equation has been obtained as

$$\left( \frac{x_0}{D_j} \right)_{\text{concentration}} = 1 + 30 \left( \frac{\rho_j}{\rho_e} \right)^{1/4} M_j^2 \left\{ 1 + M_j^2 \exp \left[ - \frac{\left( 1 - \frac{M_e}{M_j} \right)^2}{2} \right] \right\}^{-2} \quad (16)$$

From equation (16), when  $M_j = 0$ ,

$$\left( \frac{x_0}{D_j} \right)_{\text{concentration}} = 1.0$$

which corresponds to the axisymmetric wake, and the result of  $x_0/D_j = 1.0$  is supported by the data of the supersonic wake studies (refs. 18, 19, and 20). When  $M_e = 0$ , which corresponds to the jet injected into the quiescent atmosphere, the data of Keagy and Weller (ref. 21) and O'Connor (ref. 22) are fairly well correlated as seen in this figure.

Now the turbulent diffusion coefficient, assuming that it is only a function of  $x$ , can be described with the aid of equations (14) and (15) as

$$\rho D_t = (\rho D_t)_t = 0.6 \frac{\lambda^{1/2}}{\bar{x}_0} r_{mc}(\rho u)_t \quad (17)$$

It is noticeable that equation (17) does not include any adjustable constant to match the numerical solutions of wake equations with the experimental data. Such constants were included in all previous viscosity models suggested by Prandtl, Ferri, Schetz, and others.

As shown subsequently the diffusion model given by equation (17) provides good numerical predictions for the high-speed mixing of hydrogen and air, for which the decay exponent  $n$  satisfied equation (15) approximately. However, for the general case of arbitrary dissimilar gases, it has been found necessary (by means of numerical calculations) to include a molecular-weight factor given as  $1 + 0.8(W_j/W_e)$  in the expression for turbulent diffusivity; thus,

$$\rho D_t = \frac{0.6}{1 + 0.8W} \frac{\lambda^{1/2}}{\bar{x}_0} r_{mc}(\rho u)_t \quad (18)^1$$

where

$$\bar{x}_0 = 2 + 60 \left( \frac{\rho_j}{\rho_e} \right)^{1/4} M_j^2 \left\{ 1 + M_j^2 \exp \left[ - \frac{\left( 1 - \frac{M_e}{M_j} \right)^2}{2} \right] \right\}^{-2}$$

Since the ratio of the molecular weights  $W = W_j/W_e$  is very small for the mixing of light gas and heavy gas, equation (18) becomes of the same form as equation (17) as, for example, in the case of hydrogen-air mixing.

It is important to realize that the model chosen is based on the potential core derived from a step profile. Therefore, one cannot expect it to work if the initial profile consists of a boundary-layer profile. However, these difficulties could be avoided by always starting with an initial step profile, and calculating the length of the potential core for the step profile. This distance should be added to the calculations performed with the boundary-layer type profile. This procedure will result in a shift of the curve, which will indicate a slower mixing region. This fact will be evident in some of the results that will be given in the next section.

## Application to the Numerical Solution of Wake Equations

### Without Pressure Gradients

In order to investigate the validity of the present diffusion model, the wake equations have been solved for the cases without pressure gradients. The wake equations

---

<sup>1</sup> For numerical calculation, the concentration half-radius  $r_{mc}$  should be determined by the numerical procedure instead of equation (12), which will provide the analytical prediction of the half-radius in the far wake region only.

in the general form are written in the modified von Mises plane as follows:

Momentum equation:

$$\frac{\partial \bar{u}}{\partial \xi} = \frac{1}{\tau} \frac{\partial}{\partial \tau} \left( \frac{\bar{\rho} \bar{\mu}_t \bar{u} \bar{r}^2}{\tau} \frac{\partial \bar{u}}{\partial \tau} \right) - \frac{\bar{u}}{u_e} \frac{\partial u_e}{\partial \xi} \left( 1 - \frac{1}{\bar{\rho} \bar{u}^2} \right) \quad (19)$$

Energy equation:

$$\begin{aligned} \frac{\partial \bar{T}}{\partial \xi} = & \frac{1}{\tau \bar{c}_p} \frac{\partial}{\partial \tau} \left( \frac{\bar{\rho} \bar{\mu}_t \bar{c}_p \bar{u} \bar{r}^2}{Pr_t \tau} \frac{\partial \bar{T}}{\partial \tau} \right) + (\gamma_e - 1) M_e^2 \left[ \frac{\bar{T} - 1}{\bar{\rho} \bar{c}_p u_e} \frac{\partial u_e}{\partial \xi} + \frac{\bar{\rho} \bar{\mu}_t \bar{r}^2 \bar{u}}{\bar{c}_p \tau^2} \left( \frac{\partial \bar{u}}{\partial \tau} \right)^2 \right] \\ & + \frac{\bar{\rho} \bar{\mu}_t \bar{r}^2 \bar{u}}{Sc_t \bar{c}_p \tau^2} \frac{\partial \bar{T}}{\partial \tau} \sum_k \bar{c}_p \frac{\partial Y_k}{\partial \tau} \end{aligned} \quad (20)$$

Species equation:

$$\frac{\partial Y_k}{\partial \xi} = \frac{1}{\tau} \frac{\partial}{\partial \tau} \left( \frac{\bar{\rho} \bar{\mu}_t \bar{u} \bar{r}^2}{Sc_t \tau} \frac{\partial Y_k}{\partial \tau} \right) \quad (k = 1, 2, \dots) \quad (21)$$

where the modified von Mises transformation is defined by

$$\frac{\partial \tau^2}{\partial \bar{r}} = \bar{\rho} \bar{u} \bar{r}$$

$$\frac{\partial \tau^2}{\partial \bar{x}} = -\bar{\rho} \bar{v} \bar{r}$$

$$\xi = \frac{1}{4} \int_{\bar{x}_1}^{\bar{x}} Re^{-1} d\bar{x}$$

and  $\mu_t = Sc_t \rho D_t$  and  $Pr_t = Le_t Sc_t$  are used.

The associated initial and boundary conditions are

$$\bar{u}(0, \tau) = \bar{u}_i(\tau)$$

$$\bar{T}(0, \tau) = \bar{T}_i(\tau)$$

$$Y_j(0, \tau) = Y_{ji}(\tau)$$

$$\frac{\partial}{\partial \tau} \bar{u}(\xi, 0) = \frac{\partial}{\partial \tau} \bar{T}(\xi, 0) = \frac{\partial}{\partial \tau} Y_j(\xi, 0) = 0$$

$$\lim_{\tau \rightarrow \infty} \bar{u}(\xi, \tau) = \lim_{\tau \rightarrow \infty} T(\xi, \tau) = 1.0$$

$$\lim_{\tau \rightarrow \infty} Y_j(\xi, \tau) = 0$$

The numerical calculations for equations (19) to (21) were carried out by an implicit finite-difference scheme. The details of this numerical process have been reported in references 23 and 24. Also, some pertinent results relating to this program have been reported in references 25 to 27.

Once initial and boundary conditions are specified, equations (19) to (21) can be solved with the aid of equation (18) for diffusion coefficient and with the assumptions of appropriate constant values for  $Sc_t$  and  $Pr_t$ . In this present calculation,  $Sc_t = Pr_t = 0.8$  and  $Le_t = 1.0$  have been used.

The numerical calculations were carried out for the experimental data of Chriss (ref. 12) and Alpinieri (ref. 2). In figure 4, the numerical solutions for the data of Chriss are shown compared with the experimental data which were measured in hydrogen and air mixing. The accuracy of those experiments have been found to be very good by Zelazny et al. (ref. 9) and Harsha (ref. 10) (reportedly within 4 percent). Since the lateral profiles measured at several stations of  $x$  were reported in reference 12, the initial profiles for this numerical calculation were chosen at the position of  $\bar{x}_1$  indicated in figures instead of the assumed profiles at the jet exit plane.

Figures 4(a), 4(c), and 4(f) show very good agreement of numerical solutions with the experiment for concentration decay on the center line and for the concentration half-radius. Figure 4(e) shows an example for the lateral concentration profiles which agree quite well with the experimental data. Also in figures 4(a), 4(c), and 4(f) the analytical predictions of concentration half-radius  $r_{mc}$  given by equation (12) are shown. The agreement with the experimental data is excellent, considering that equation (12) does not include any adjustable constant to match the solutions with data.

Concerning the velocity profiles for the data of Chriss (ref. 12), the center-line profile and the half-radius have been predicted well as seen in figures 4(b), 4(d), and 4(g). These results prove that if there is no pressure gradient in the flow field the assumptions of  $Sc_t = Pr_t = 0.8$  and  $Le_t = 1.0$  are valid for the high-speed mixing of hydrogen and air.

In figures 4(c) and 4(f), the numerical solutions obtained by employing the eddy-viscosity model of reference 1 are presented. The comparisons with the data show that the Ferri model provides fairly good predictions in the far wake region.

The numerical result for the data of Alpinieri (ref. 2), which are characterized by the very small momentum of the inner hydrogen jet, is shown in figure 5. The result given by the present diffusion model agrees fairly well with the data.

In figure 6, the results are shown for the case of  $CO_2$  and air mixing measured by Alpinieri. In these cases numerical results agree fairly well with the data which have the decay exponent  $n \approx 1.5$ .

Throughout these numerical computations the momentum integral of the wake has been checked at each station of finite-difference calculation and found to be constant with a variation of less than  $\pm 1$  percent.

## COMPARISONS WITH SELECTED CASES

In addition to the cases presented in the previous section of this report, six cases (identified as 9, 10, 11, 12, 20, and 21) will be chosen for this section. Each of these cases will be discussed separately. An additional case was chosen in order to evaluate the numerical techniques used in the analysis. Table I presents initial conditions for all the above-mentioned cases.

### Discussion of the Results of Selected Cases

Additional case.- For the additional case (see page 735 for explanation), a step profile has been given for the velocity as well as the concentration. The velocity did not present any problem; however, the concentration profile had to be rounded off slightly in order to start the calculation. For this case, the transformed  $\bar{r}$  coordinate, which is indicated as  $\tau$ , had a step size of  $\Delta\tau$  equal to 0.009. The total number of grid points in the  $\tau$ -direction was 60. The total time required for the calculation on the 6600 computer at NYU was 180 seconds. The results of this case are shown in figure 7.

Case 9.- In case 9, the analysis was carried out for the experimental conditions of Forstall and Shapiro (ref. 11). Initial profiles were given both for the velocity and concentration. However, one could hardly consider this case as the mixing of two dissimilar gases since the center jet contained  $1\frac{1}{2}$  percent, by mass, of a helium tracer gas.

The momentum controls the mixing in this case, and therefore it dominates the mixing primarily. The results of the present analysis are presented in figure 8 and compared with the experimental results. It is noticed that the Ferri model, which essentially reduces to the Prandtl model for low speeds, has the best agreement with the experimental results.

Case 10.- In case 10 (see ref. 12) the initial profiles were given, and therefore no adjustments were needed. Figure 9 presents results of the Ferri model as well as the results of the present model. Both models seem to agree initially; however, the present model seems to give the correct trend of the experimental results. For this case, even though the flow is subsonic, the analysis still agrees excellently with the experimental results.

Case 11.- The results for case 11 are presented in figure 10. The center jet in this case is a subsonic air stream traveling at Mach 0.90 surrounded by an annular Mach 1.3 nozzle. In this case, a 1-percent ethylene tracer gas was mixed into the central stream. As far as the mixing is concerned, this was a predominantly momentum transfer, and

therefore the analysis which is presented herein and which has been derived from a concentration potential core would hardly be suitable. However, the analysis was still carried out for this model. Two different initial conditions were chosen for case 11:

- (a) Assuming an initial step profile
- (b) Assuming the initial profile provided

It is clearly seen that condition (a) provides the fastest mixing, and the boundary-layer type profile (condition (b)) results in a slower mixing region. In order to use this model for the potential core, the length required to reach the boundary-layer profile should be added as initial conditions, since the analysis here assumes a step profile. The results of such a correction are included in figure 10 and labeled "New model with correction." Even though the analysis of such a technique improves the agreement, it still falls short of the experimental results.

Case 12.- The results for case 12 are presented in figure 11. The center jet is entirely H<sub>2</sub> at a Mach number of 0.89. As seen in figure 11, the present analysis agrees fairly well with the experimental results; however, the Ferri model falls quite short of the experimental results.

Case 20.- In case 20, only a 2 percent by volume of H<sub>2</sub> was placed in the center jet, and therefore the mixing is dominated by momentum. The results for this case are presented in figure 12, which shows no agreement with the experimental results.

Case 21.- The center jet is entirely H<sub>2</sub> for case 21, and both inside and outside streams are subsonic. The results for this case are presented in figure 13, and the analysis, as expected, is in fair agreement with the experimental results.

#### Summary of Results of Selected Cases

The following general results were noted for the cases selected:

- (1) For all the cases where a lighter molecular gas such as H<sub>2</sub> or He is placed in the center, the present analysis works very well (that is,  $\lambda < 1$ ). This is independent of the conditions whether the flow is subsonic or supersonic.
- (2) For low-speed flows, where  $\lambda > 1$  (predominantly flows of air-to-air mixing), the Ferri model seems to work best.
- (3) As noted previously, the decay such as exists for the flow described in result (1) is always proportional to  $x^{-2}$ .

#### CONCLUSIONS

A model has been presented for the prediction of the concentration decay for high-speed coaxial mixing. The model has been derived from accurate correlation of data

derived from the length of the concentration potential core. Comparisons of this model with available experimental results seem to indicate good agreement, except for cases where the mass-flow ratio is greater than 1 (mixing of gases having approximately the same molecular weight). For all the cases where the gas in the center was much lighter than the coflowing outer gas, the analyses predicted the concentration decays excellently. It is indicated in this paper that no single model could solve the problem of mixing, and attempts should be made to analyze each problem separately. In addition, differentiation should be made between momentum, mass, and thermal diffusion. These effects become much more important when pressure gradients are present in the flow field.

## REFERENCES

1. Ferri, A.; Libby, P. A.; and Zakkay, V.: Theoretical and Experimental Investigation of Supersonic Combustion. High Temperatures in Aeronautics, Carlo Ferrari, ed., Pergamon Press, Inc., 1964, pp. 55-118.
2. Alpinieri, Louis J.: Turbulent Mixing of Coaxial Jets. AIAA J., vol. 2, no. 9, Sept. 1964, pp. 1560-1567.
3. Ting, Lu; and Libby, Paul A.: Remarks on the Eddy Viscosity in Compressible Mixing Flows. J. Aero/Space Sci., vol. 27, no. 10, Oct. 1960, pp. 797-798.
4. Donaldson, Coleman duP.; and Gray, K. Evan: Theoretical and Experimental Investigation of the Compressible Free Mixing of Two Dissimilar Gases. AIAA J., vol. 4, no. 11, Nov. 1966, pp. 2017-2025.
5. Peters, C. E.: Turbulent Mixing and Burning of Coaxial Streams Inside a Duct of Arbitrary Shape. AEDC-TR-68-270, U.S. Air Force, Jan. 1969. (Available from DDC as AD 680 397.)
6. Zakkay, Victor; Krause, Egon; and Woo, Stephen D. L.: Turbulent Transport Properties for Axisymmetric Heterogeneous Mixing. AIAA J., vol. 2, no. 11, Nov. 1964, pp. 1939-1947.
7. Schetz, Joseph A.: Turbulent Mixing of a Jet in a Coflowing Stream. AIAA J., vol. 6, no. 10, Oct. 1968, pp. 2008-2010.
8. Clauser, Francis H.: The Turbulent Boundary Layer. Vol. IV of Advances in Applied Mechanics, H. L. Dryden and Th. von Kármán, eds., Academic Press, Inc., 1956, pp. 1-51.
9. Zelazny, S. W.; Morgenthaler, J. H.; and Herendeen, D. L.: Reynolds Momentum and Mass Transport in Axisymmetric Coflowing Streams. Proceedings of the 1970 Heat Transfer and Fluid Mechanics Institute, Turgut Sarpkaya, ed., Stanford Univ. Press, c.1970, pp. 135-152.
10. Harsha, Philip Thomas: Free Turbulent Mixing: A Critical Evaluation of Theory and Experiment. AEDC-TR-71-36, U.S. Air Force, Feb. 1971. (Available from DDC as AD 718 956.)
11. Forstall, Walton, Jr.; and Shapiro, Ascher H.: Momentum and Mass Transfer in Coaxial Gas Jets. J. App. Mech., vol. 17, no. 4, Dec. 1950, pp. 399-408.
12. Chriss, D. E.: Experimental Study of the Turbulent Mixing of Subsonic Axisymmetric Gas Streams. AEDC-TR-68-133, U.S. Air Force, Aug. 1968. (Available from DDC as AD 672 975.)

13. Peters, C. E.; Chriss, D. E.; and Paulk, R. A.: Turbulent Transport Properties in Subsonic Coaxial Free Mixing Systems. AIAA Paper No. 69-681, June 1969.
14. Zakkay, Victor; and Krause, Egon: Mixing Problems With Chemical Reactions. Supersonic Flow Chemical Processes and Radiative Transfer, D. B. Olfe and V. Zakkay, eds., Pergamon Press, Inc., 1964, pp. 3-29.
15. Zakkay, V.; Sinha, R.; and Fox, H.: Some Remarks on Diffusion Processes in Turbulent Mixing. AIAA J., vol. 6, no. 7, July 1968, pp. 1425-1427.
16. Libby, Paul A.: Theoretical Analysis of Turbulent Mixing of Reacting Gases With Application to Supersonic Combustion of Hydrogen. ARS J., vol. 32, no. 3, Mar. 1962, pp. 388-396.
17. Kleinstein, Gdalia: Mixing in Turbulent Axially Symmetric Free Jets. J. Spacecraft & Rockets, vol. 1, no. 4, July-Aug. 1964, pp. 403-408.
18. Martellucci A.; Trucco, H.; Ranlet, J.; and Agnone, A.: Measurements of the Turbulent Near Wake of a Cone at Mach 6. AIAA Paper No. 66-54, Jan. 1966.
19. Sinha, Ram; and Zakkay, Victor: Experimental and Theoretical Investigation of the Near Wake in an Axisymmetric Supersonic Flow With and Without Base Injection. NYU-AA-68-26, New York Univ., May 1968. (Available from DDC as AD 683 528.)
20. Sinha, Ram P.: Experimental and Theoretical Investigation of the Near Wake in an Axisymmetric Supersonic Flow With and Without Base Injection. Ph. D. Thesis, New York Univ., 1968.
21. Keagy, W. R.; and Weller, A. E.: A Study of Freely Expanding Inhomogeneous Jets. 1949 Heat Transfer and Fluid Mechanics Institute, Amer. Soc. Mech. Eng., May 1949, pp. 89-98.
22. O'Connor, T. J.; Comfort, E. H.; and Cass, L. A.: Turbulent Mixing of an Axisymmetric Jet of Partially Dissociated Nitrogen With Ambient Air. AIAA J., vol. 4, no. 11, Nov. 1966, pp. 2026-2032.
23. Fox, Herbert; Sinha, Ram; and Weinberger, Lawrence: An Implicit Finite Difference Solution for Jet and Wake Problems. Pt. I: Analysis and Test Cases. ARL 70-0025, U.S. Air Force, Feb. 1970.
24. Sinha, Ram; Fox, Herbert; and Weinberger, Lawrence: An Implicit Finite Difference Solution for Jet and Wake Problems. Pt. II: Program Manual. ARL 70-0024, U.S. Air Force, Feb. 1970. (Available from DDC as AD 707 866.)
25. Fox, Herbert; Zakkay, Victor; and Sinha, Ram: A Review of Problems in the Non-reacting Turbulent Far Wake. Astronaut. Acta, vol. 14, no. 3, Mar. 1969, pp. 215-228.

26. Zakkay, V.; Sinha, R.; and Fox, H.: An Experimental Study of Some Base Injection Techniques and the Effect of Large Pressure Gradients on Turbulent Diffusion Processes. ARL 68-0160, U.S. Air Force, Aug. 1968. (Available from DDC as AD 679 218.)
27. Zakkay, V.; and Sinha, R.: An Experimental Investigation of the Near Wake in an Axisymmetric Supersonic Flow With and Without Base Injection. Israel J. Technol., vol. 7, nos. 1-2, 1969, pp. 43-53.

TABLE I.- INITIAL CONDITIONS FOR SELECTED CASES

Test case	Jet	$x_i$	$u_j/u_e$	$\Delta\tau$ (* )	N	Profile	$\lambda$	$M_e$
Additional	H <sub>2</sub>	0.0	3.84	0.009	60	u-step $\alpha$ -step (modified)	0.262	0.681
9	He and air mixture	0.0	4.0	0.04	55	As given	3.68	0.0266
10	H <sub>2</sub>	5.932	6.3	0.03	60	As given	0.508	0.422
11	Air	0.0	0.735	0.03	55	As given	0.634	1.312
12	H <sub>2</sub>	0.0	2.726	0.03	70	As given	0.0439	1.32
20	H <sub>2</sub> and air mixture	0.4568	2.1926	0.03	55	As given	2.06	0.158
21	H <sub>2</sub>	5.15	3.078	0.03	45	As given	0.398	0.497

\*  $\Delta\tau$  step size in  $\tau$ -direction;  $\tau$  transformed  $\bar{r}$  coordinate as defined by

$$\tau = \left( \int_0^{\bar{r}} \bar{\rho} \bar{u} \, d\bar{r} \right)^{0.5} .$$

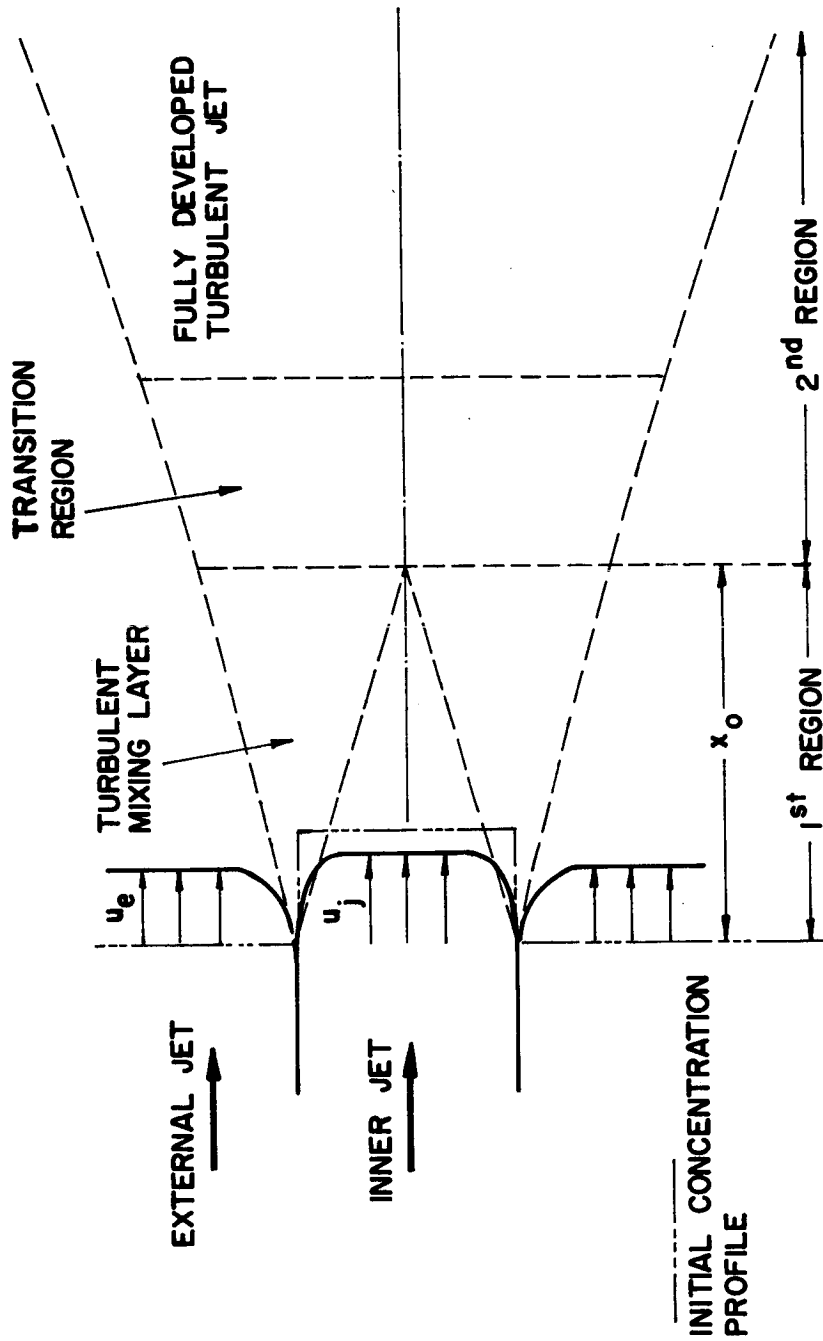


Figure 1.- Turbulent jet mixing flow model.

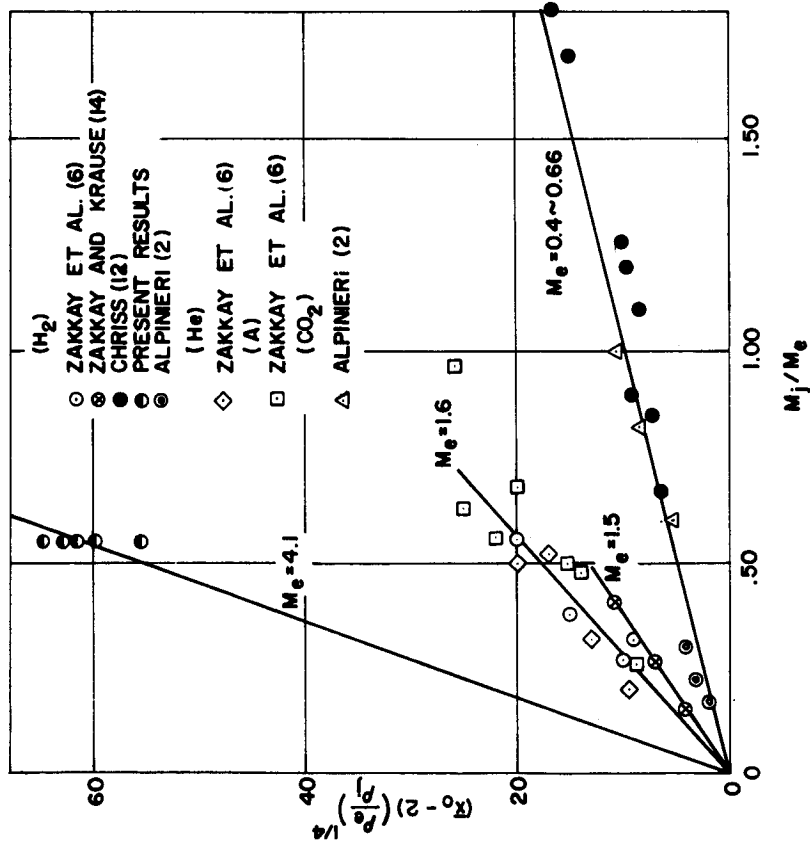


Figure 2.- Length of concentration potential core as a function of Mach number ratio.

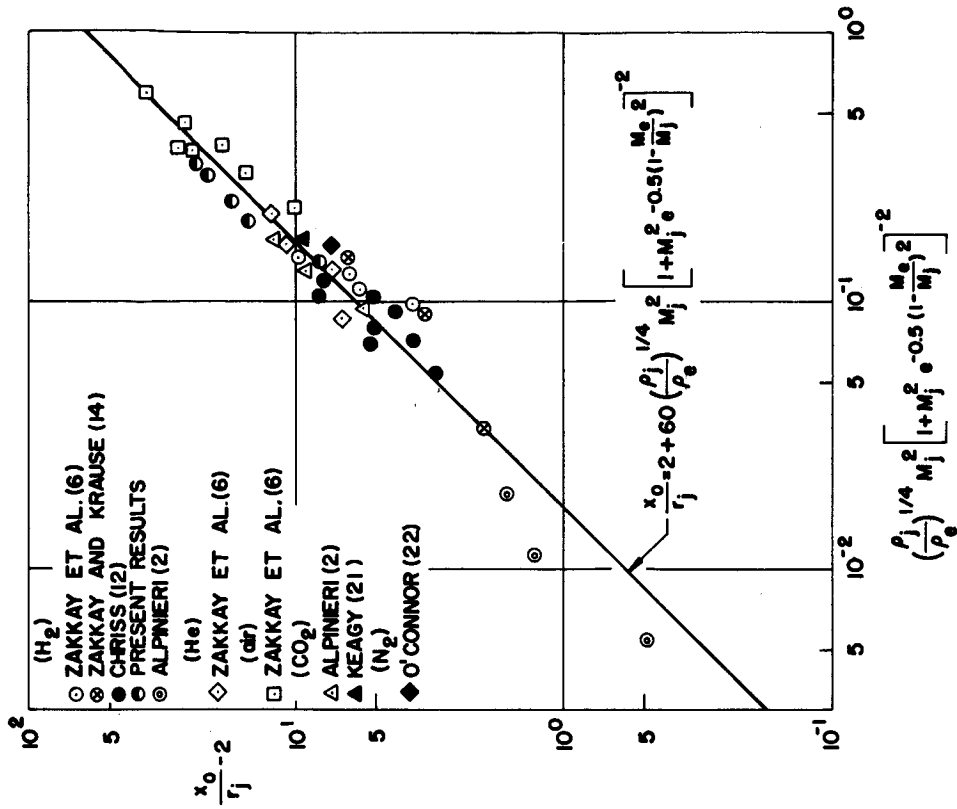


Figure 3.- Correlation for the length of concentration potential core.

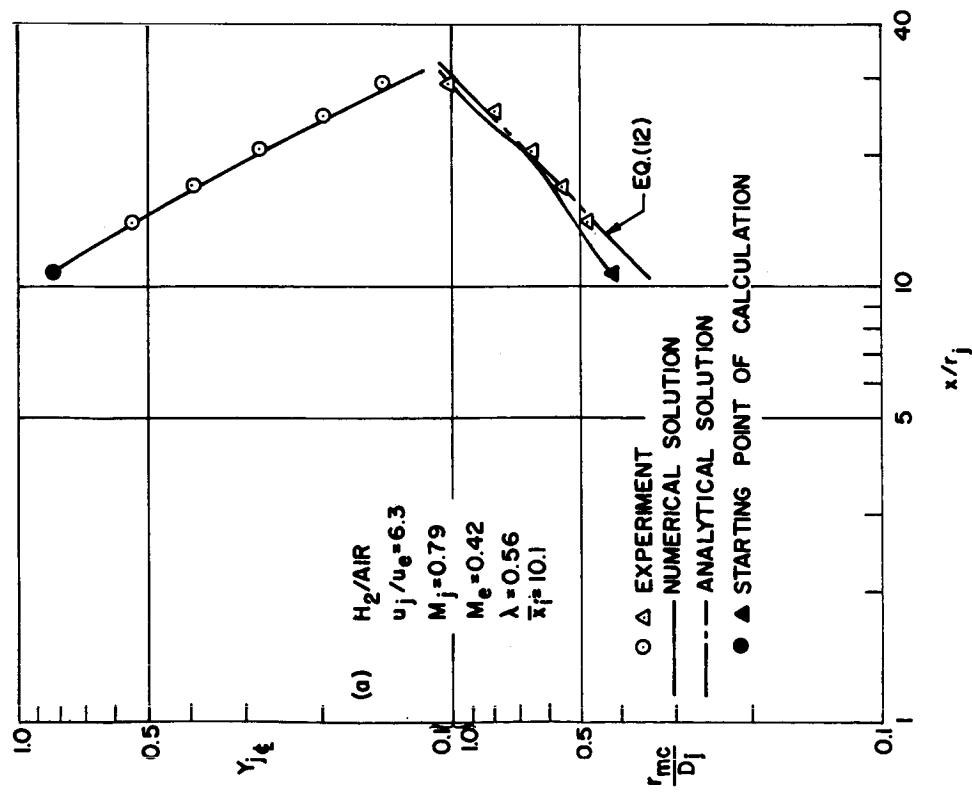
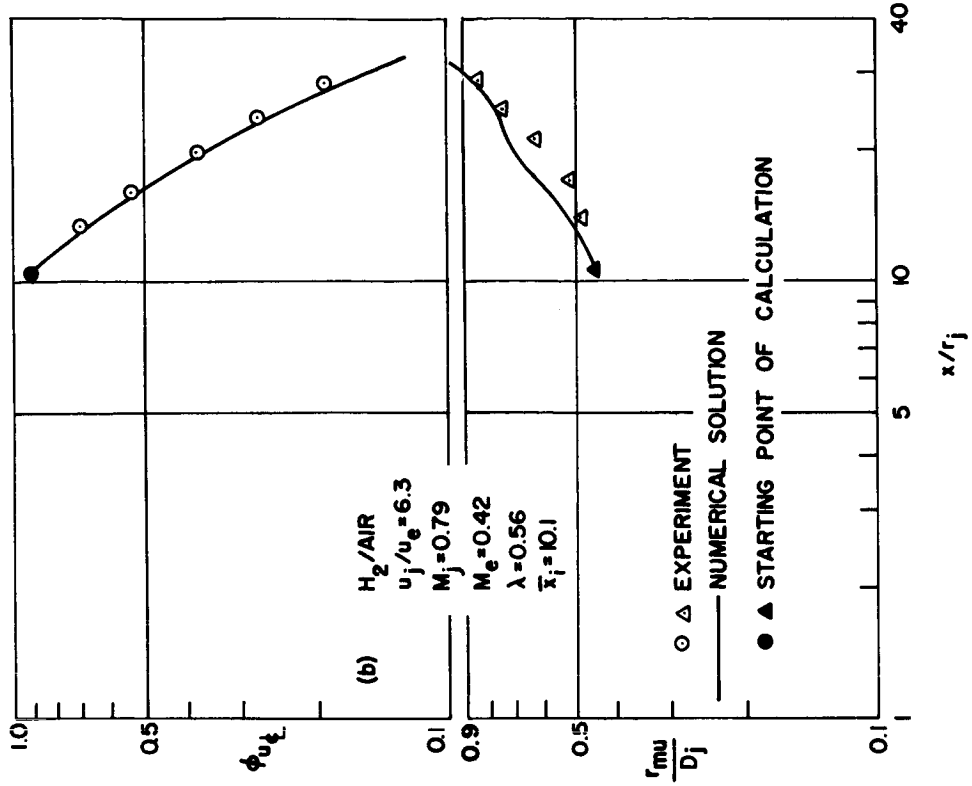


Figure 4.- Comparison of numerical results with the data of Chriss (ref. 12).

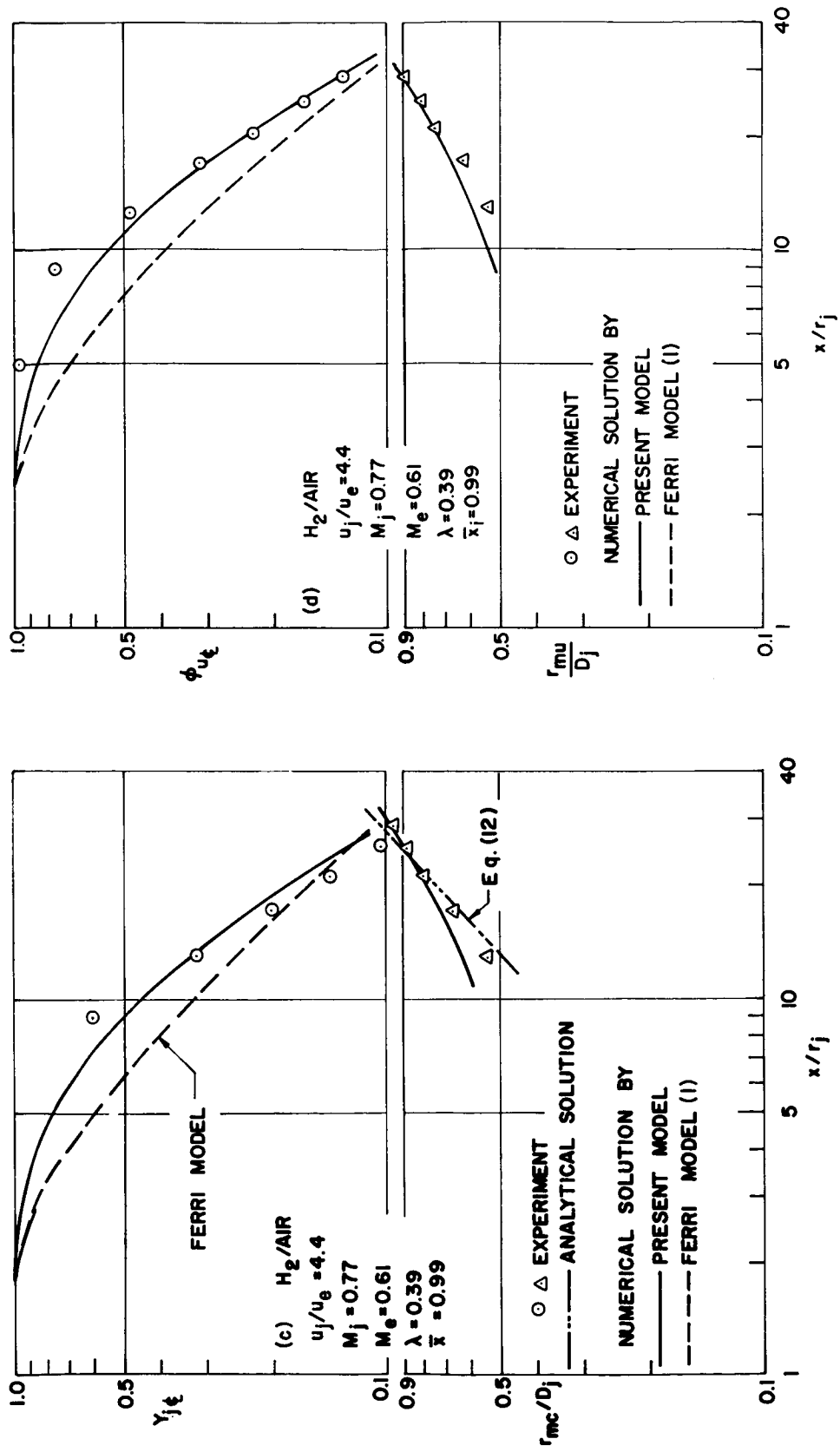


Figure 4.- Continued.

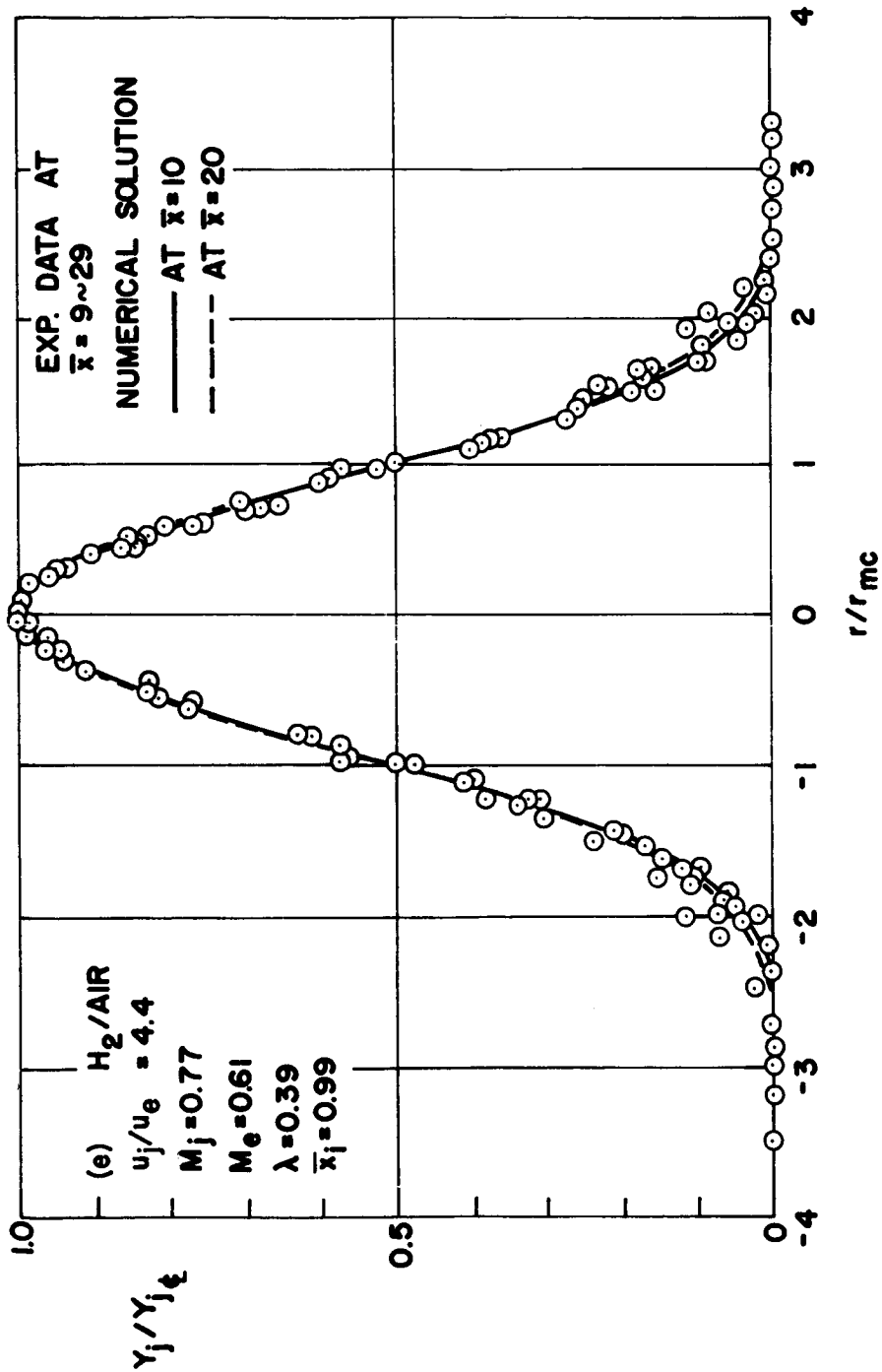


Figure 4.- Continued.

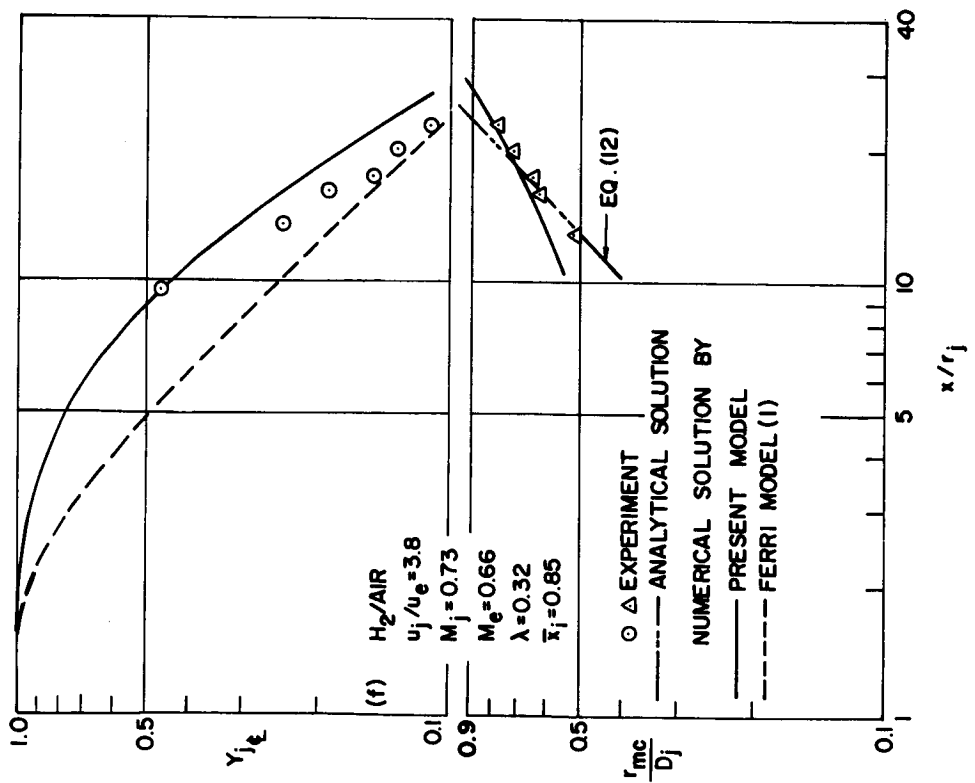
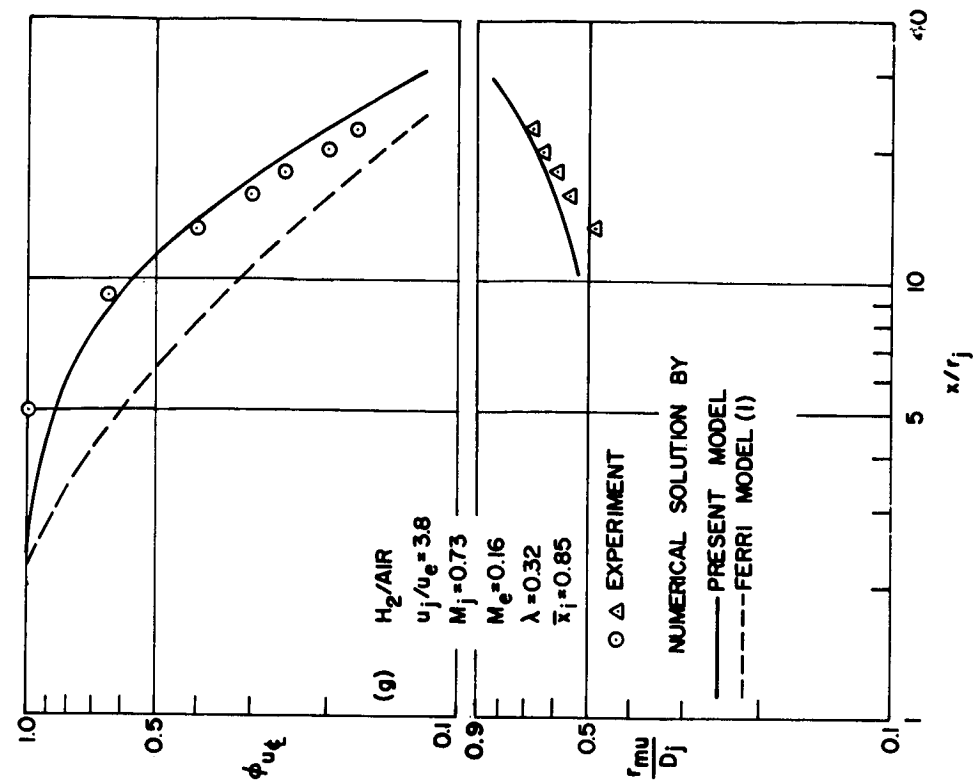


Figure 4. - Concluded.

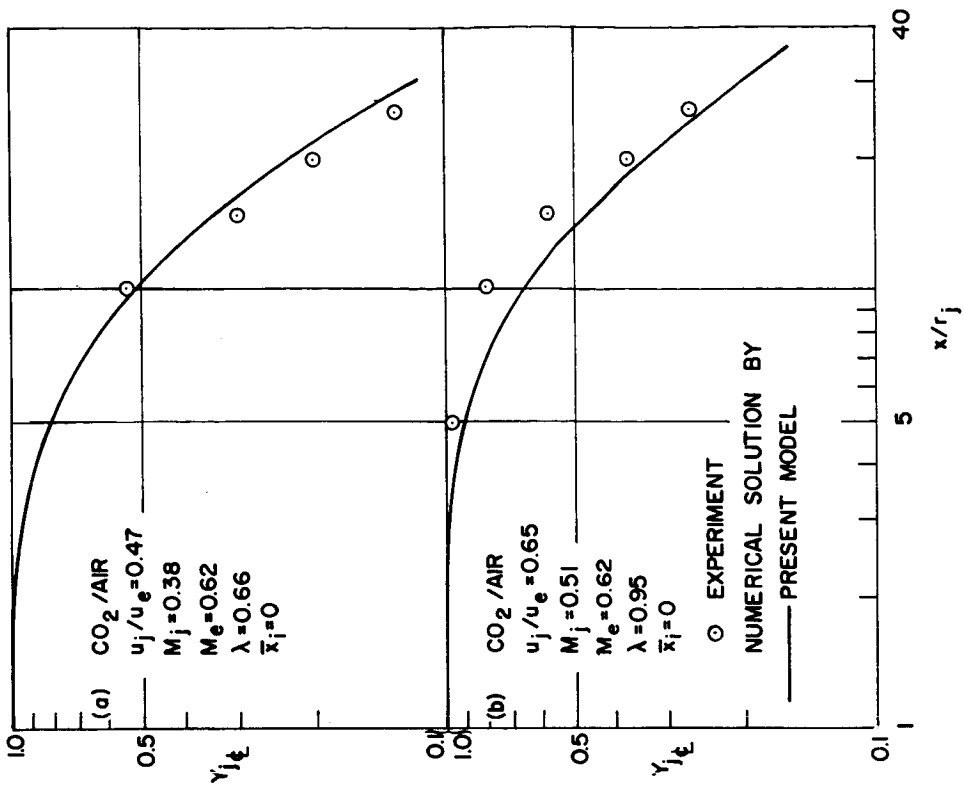


Figure 5.- Comparison of numerical results with the data of Alpinieri (ref. 2) for the mixing of hydrogen and air.

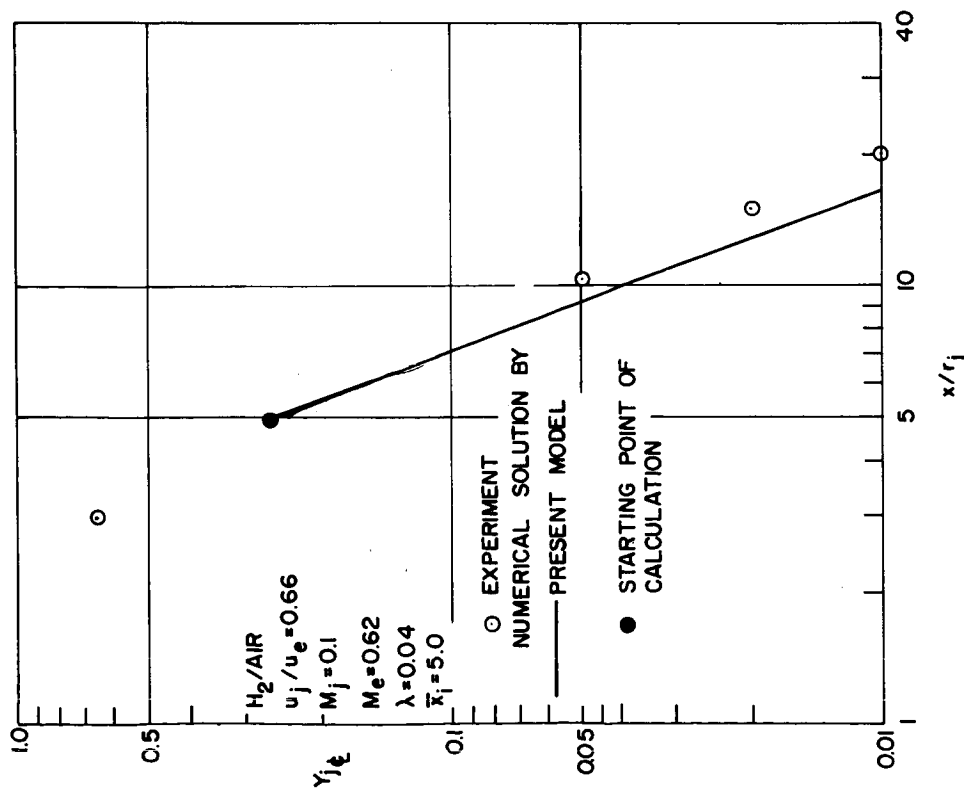


Figure 6.- Comparison of numerical results with the data of Alpinieri (ref. 2) for the mixing of carbon dioxide and air.

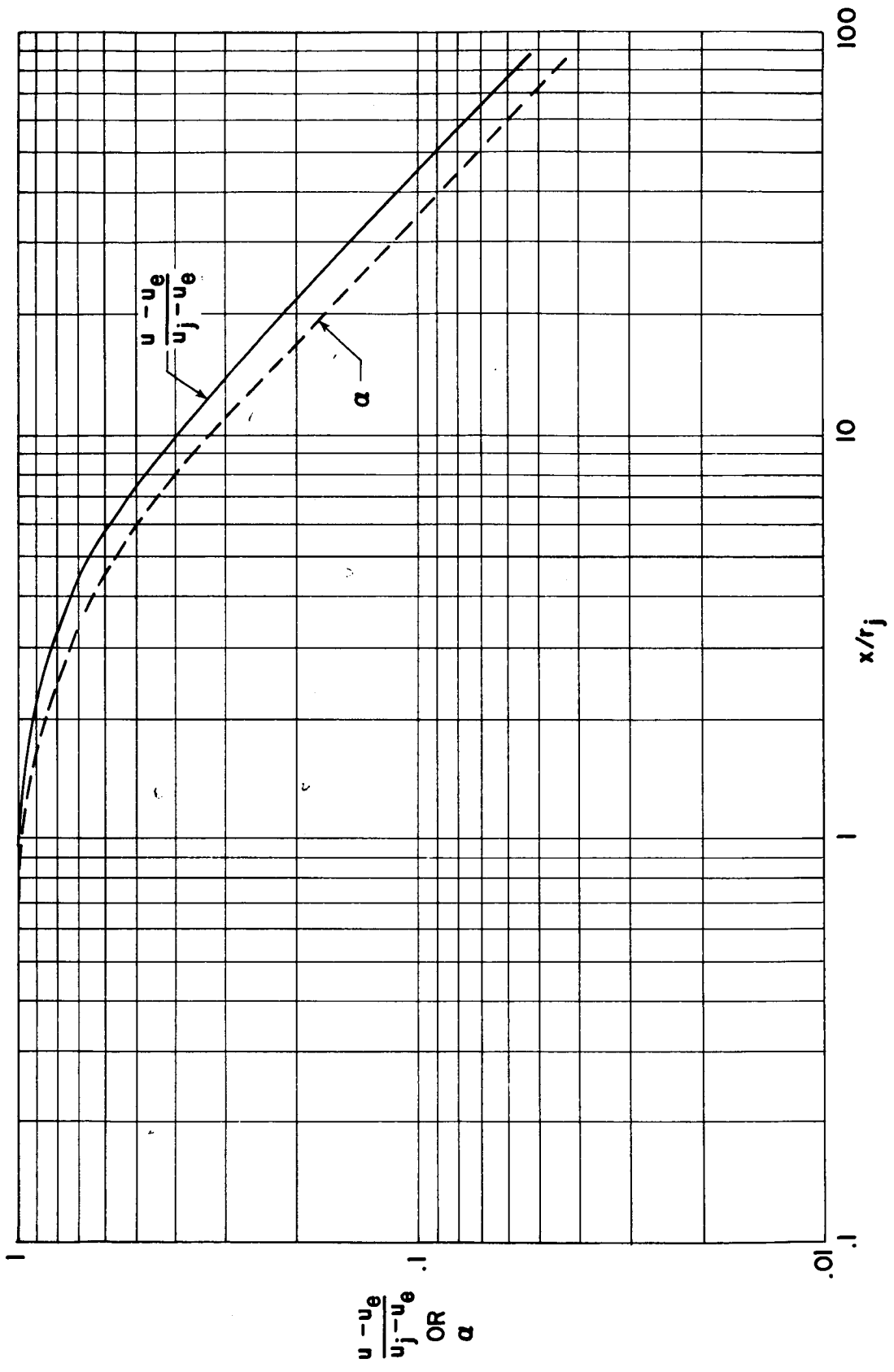


Figure 7.- Additional case.

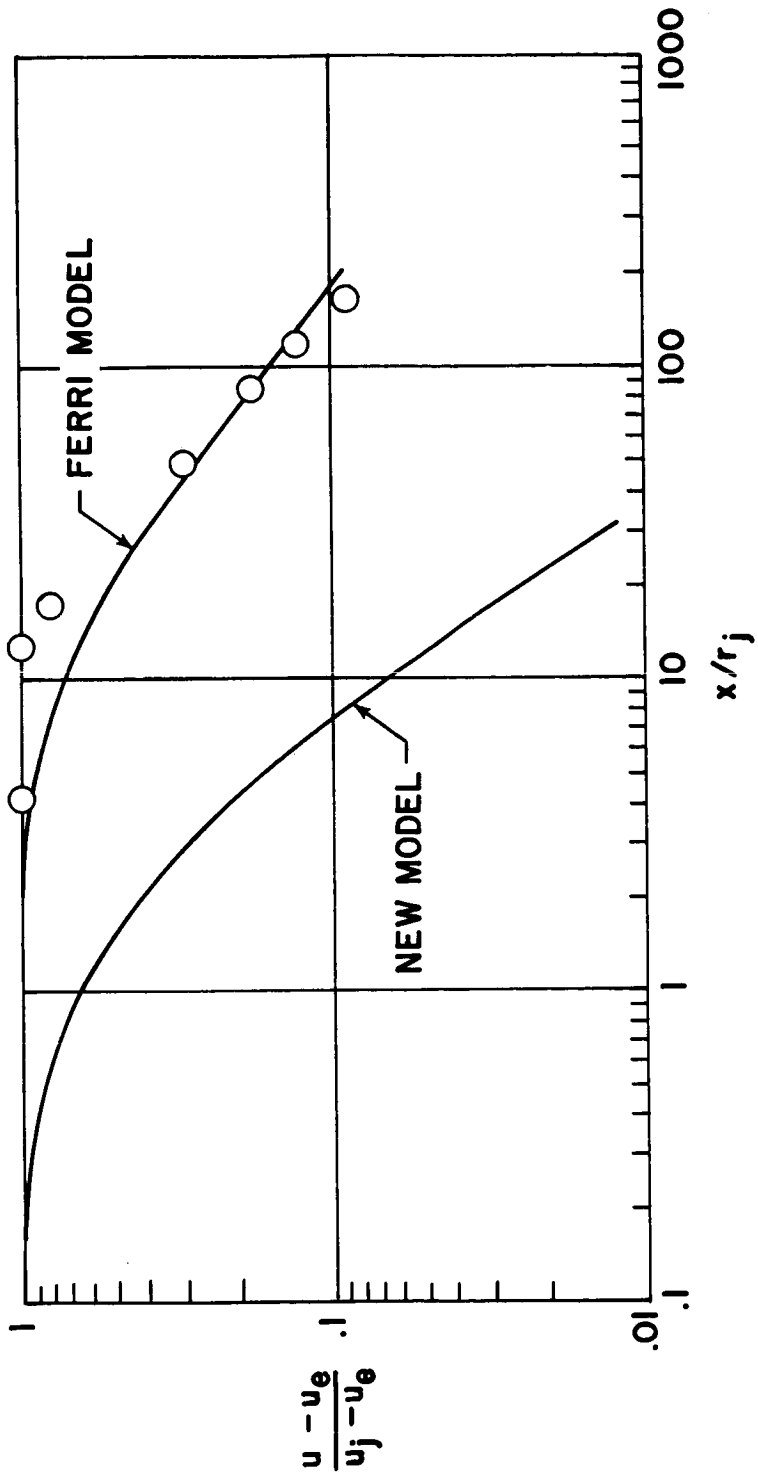


Figure 8. - Case 9.

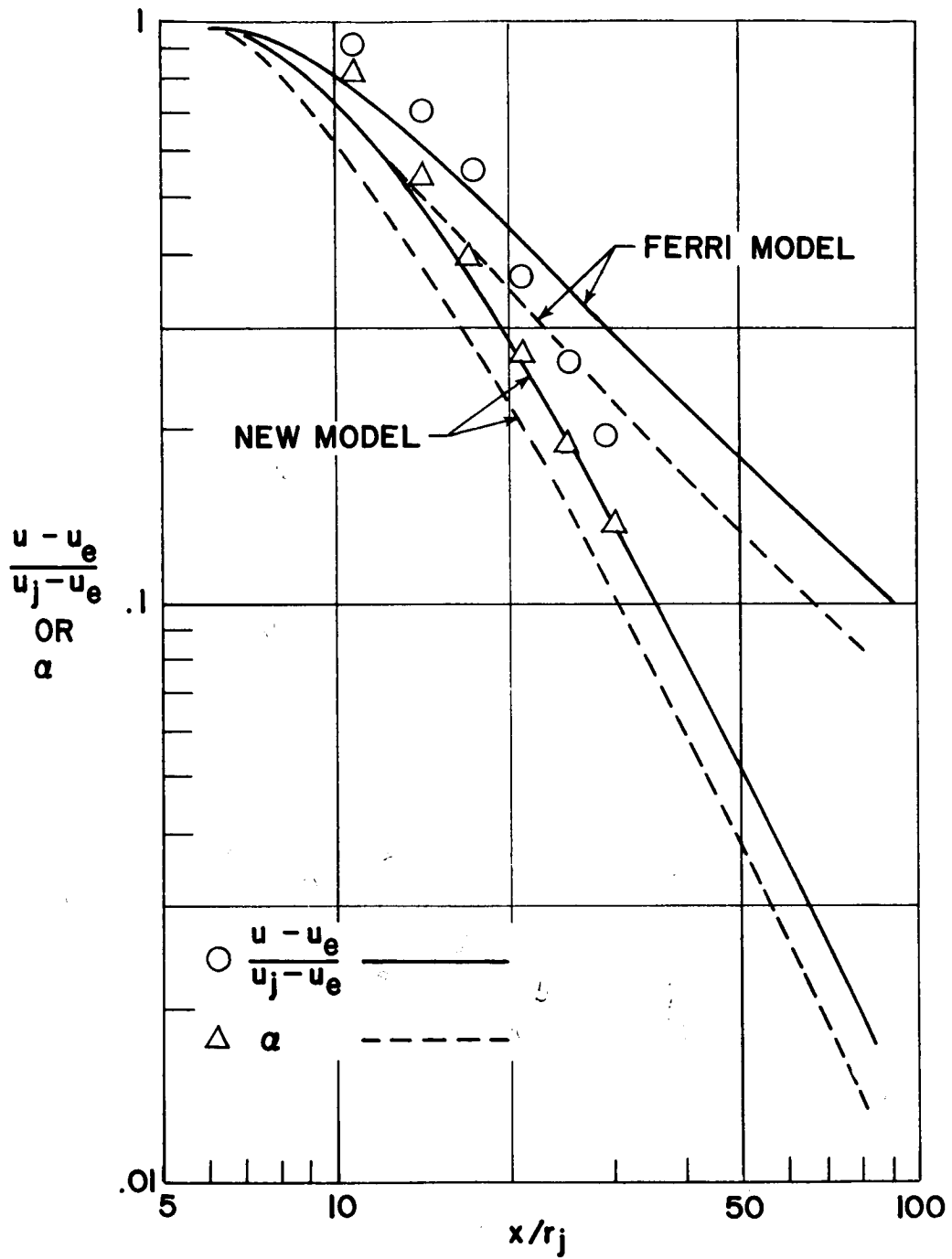


Figure 9.- Case 10.

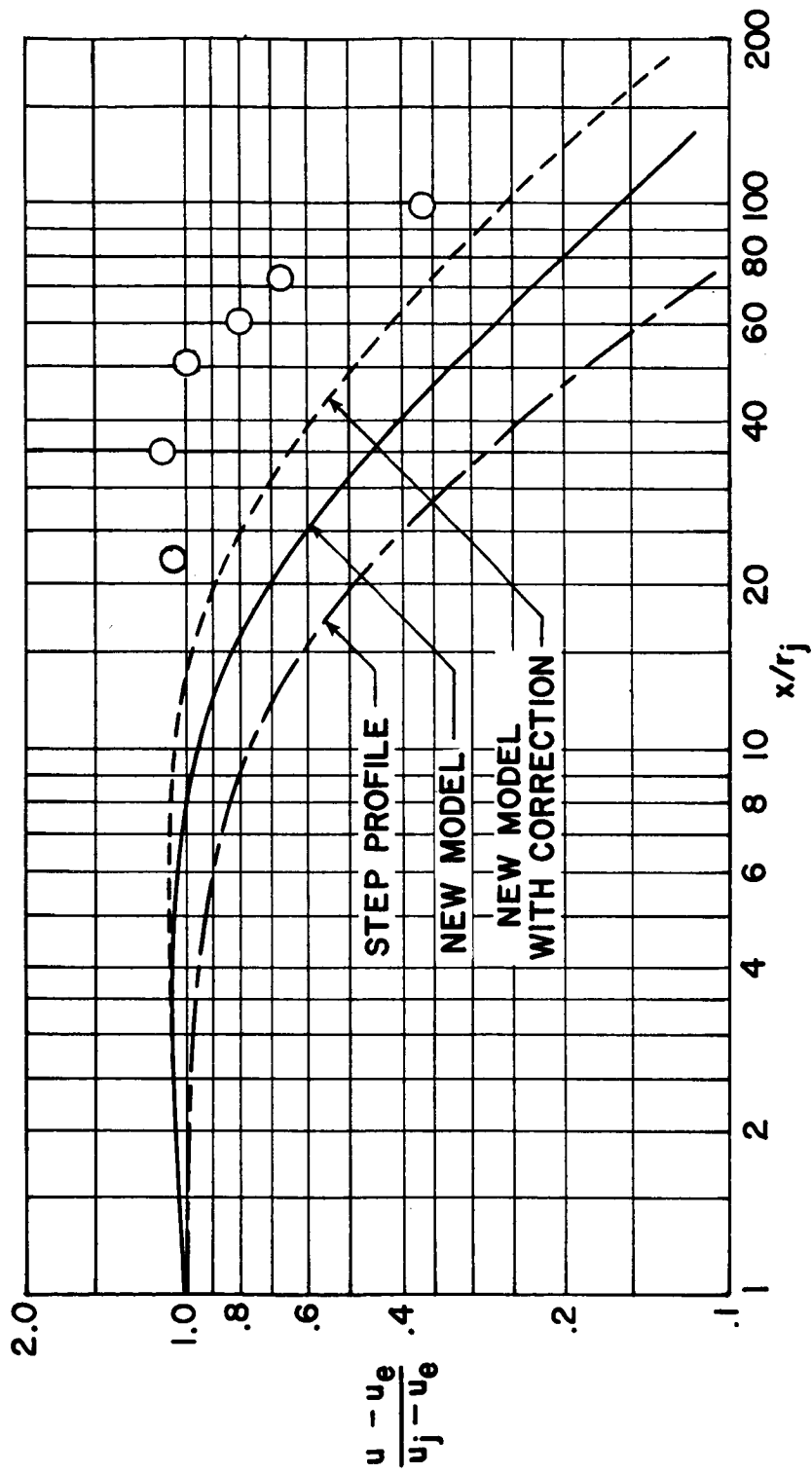


Figure 10.- Case 11.

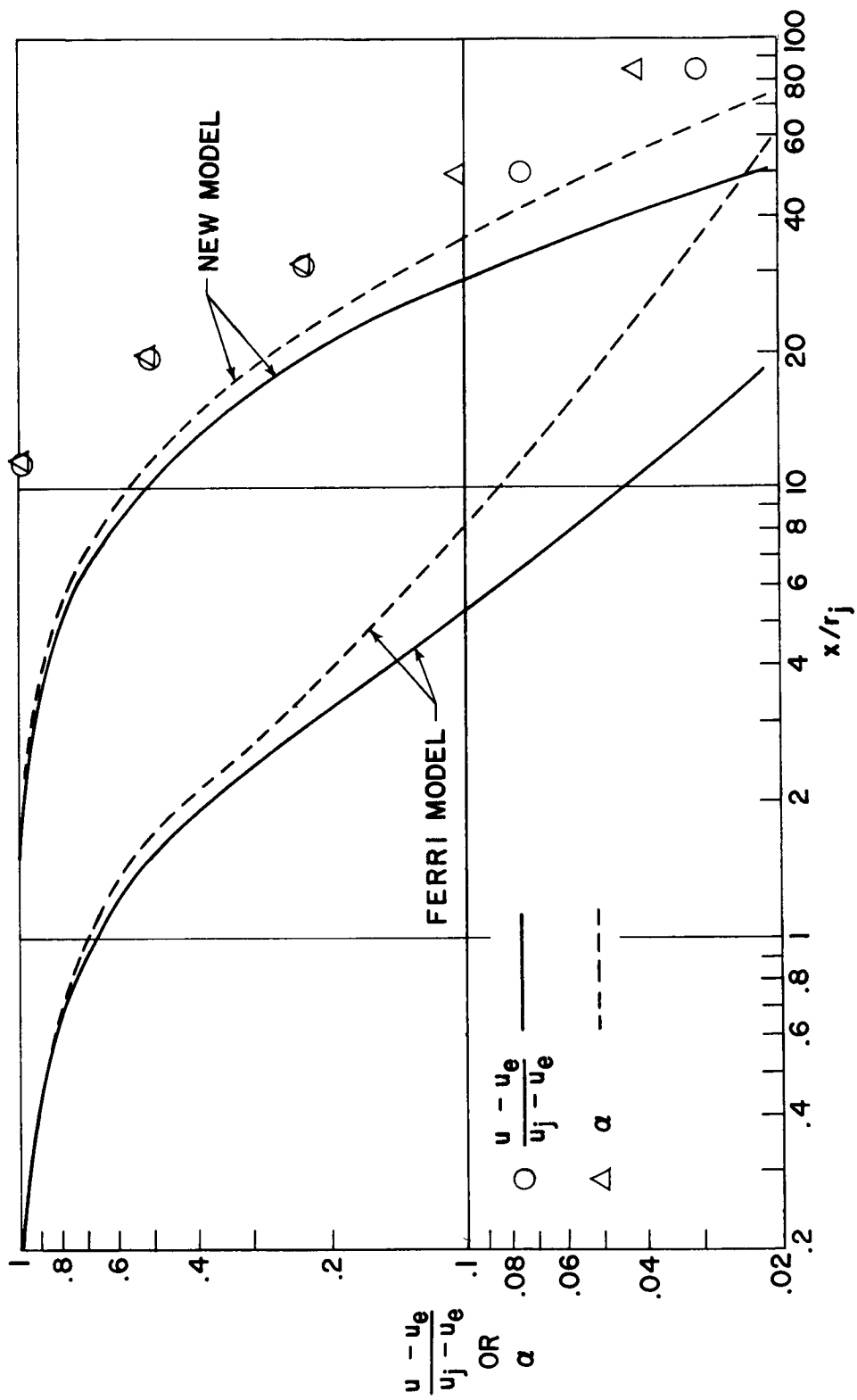


Figure 11.- Case 12.

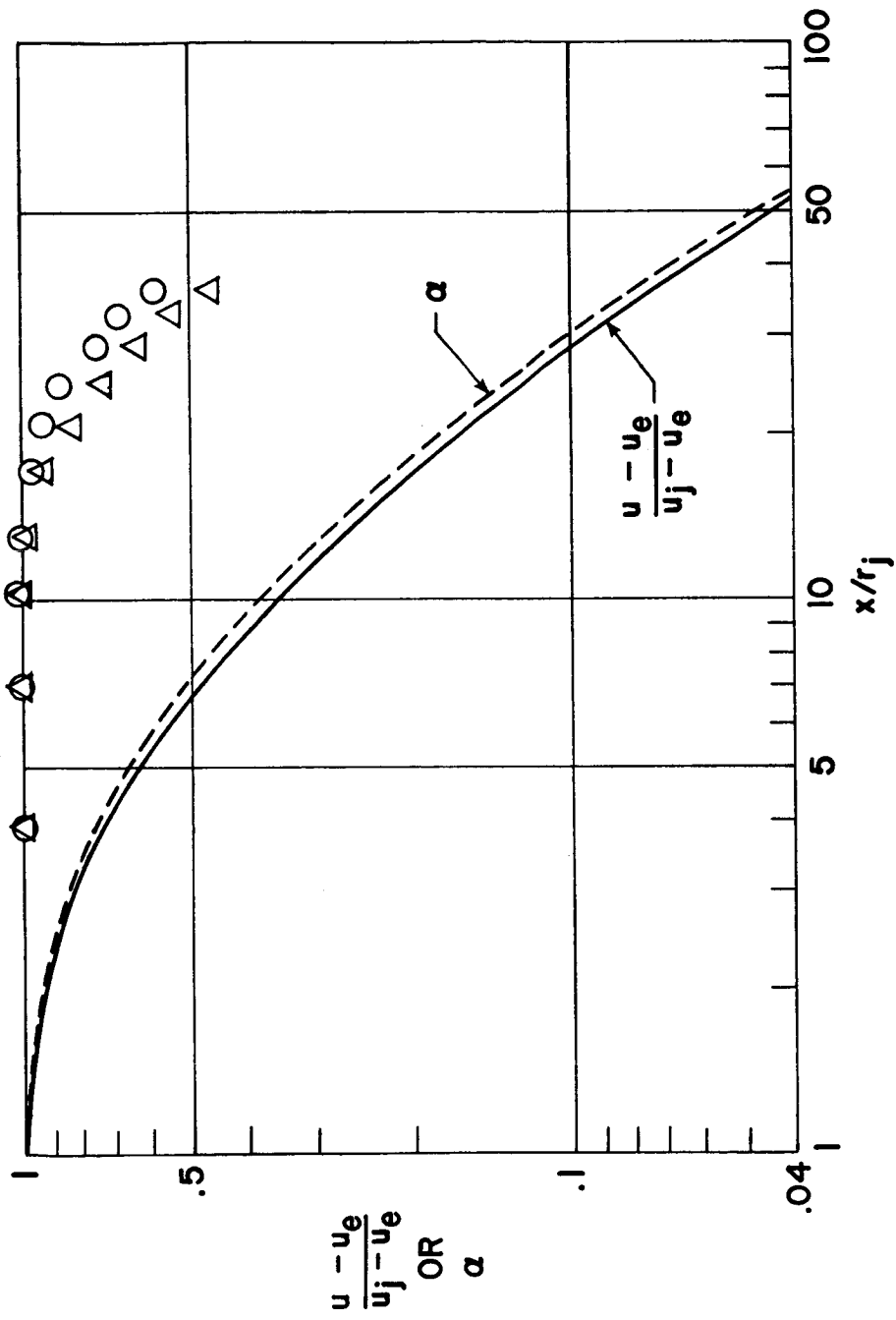


Figure 12.- Case 20.

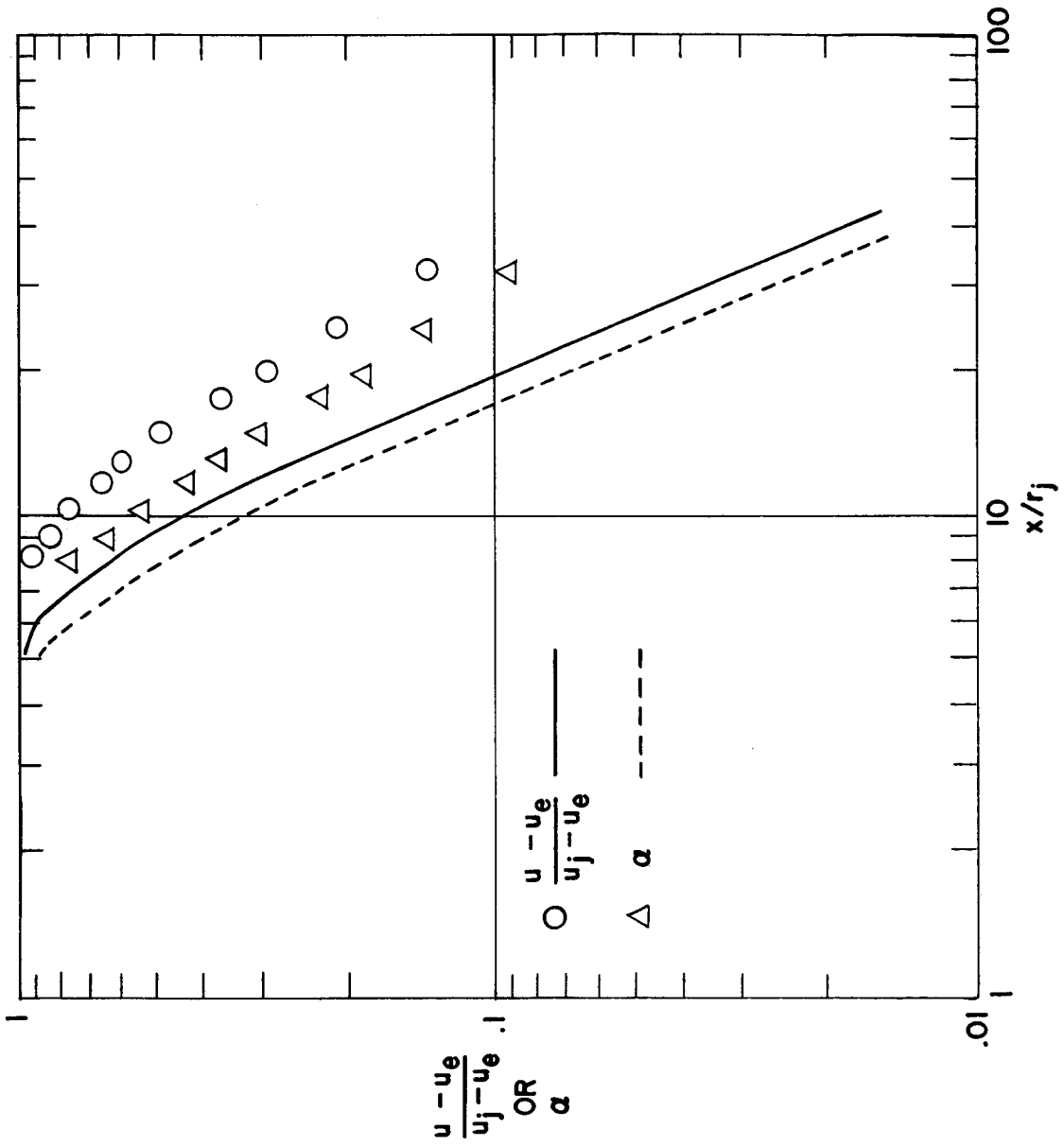


Figure 13.- Case 21.